

**A reversible carnitine palmitoyltransferase (CPT1) inhibitor offsets the proliferation of chronic lymphocytic leukemia cells**

*Elena Gugiatti,<sup>1</sup> Claudya Tenca,<sup>1</sup> Silvia Ravera,<sup>2</sup> Marina Fabbi,<sup>3</sup> Fabio Ghiotto,<sup>1,4</sup> Andrea N. Mazzarello,<sup>5</sup> Davide Bagnara,<sup>1,5</sup> Daniele Reverberi,<sup>4</sup> Daniela Zarcone,<sup>1</sup> Giovanna Cutrona,<sup>4</sup> Adalberto Ibatici,<sup>6</sup> Ermanno Ciccone,<sup>1</sup> Zbigniew Darzynkiewicz,<sup>7</sup> Franco Fais<sup>1,4</sup>\* and Silvia Bruno<sup>1</sup>\**

*<sup>1</sup>Department of Experimental Medicine, University of Genoa, Italy; <sup>2</sup>Department of Pharmacy, University of Genoa, Italy; <sup>3</sup>Biotherapies Unit, Ospedale Policlinico San Martino, Genoa, Italy; <sup>4</sup>Molecular Pathology Unit, Ospedale Policlinico San Martino, Genoa, Italy; <sup>5</sup>The Feinstein Institute for Medical Research, North Shore-Long Island, Experimental Immunology, Manhasset, NY, USA; <sup>6</sup>Hematology Unit and Bone Marrow Transplantation, Ospedale Policlinico San Martino, Genoa, Italy and <sup>7</sup>Brander Cancer Research Institute, Department of Pathology, New York Medical College, NY, USA*

*\*These authors contributed equally to the work.*

*Correspondence: [silvia.bruno@unige.it](mailto:silvia.bruno@unige.it)  
doi:10.3324/haematol.2017.175414*

TABLE S1

## CLL patient characteristics

Pts #	Binet	IG mutations status	% CD38 (30% cut-off)	VH gene	<i>TP53</i>	<i>NOTCH1</i>	<i>SF3B1</i>	Chromosomal aberrations (FISH)
1	C	M-CLL	POS	VH3-30	wt	wt	wt	del 11q22*, del 13q14**, del 17p13***
2	B	U-CLL	POS	VH1-69	wt	wt	wt	nd
3	C	M-CLL	POS	VH3-7	nd	wt	nd	nd
4	C	U-CLL	POS	VH3-48	nd	wt	wt	nd
5	B	U-CLL	NEG	VH3-11	wt	wt	wt	del 13q14
6	B	M-CLL	POS	VH4-31	wt	wt	wt	nd
7	C	U-CLL	POS	VH5-51	nd	wt	wt	nd
8	A	M-CLL	NEG	VH3-30	nd	wt	wt	nd
9	C	U-CLL	POS	VH1-69	wt	wt	wt	del 17p13, del 13q14, trisomy 12
10	C	U-CLL	POS	VH4-74	MUT	wt	wt	del 11q22, del 13q14
11	A	M-CLL	POS	VH4-34	wt	wt	wt	nd
12	C	M-CLL	POS	VH1-2*02	nd	nd	nd	del 17p13 (5%)
13	-	U-CLL	NEG	VH1-18*04	wt	nd	nd	NEG
14	A	U-CLL	POS	VH1-69*01	wt	nd	nd	del 11q22, del 13q14, del 17p13 (5%)
15	B	M-CLL	NEG	VH4-34*01	wt	nd	wt	trisomy 12
16	A	U-CLL	NEG	VH4-39*01	MUT	nd	wt	trisomy 12
17	A	M-CLL	POS	VH3-48*02	wt	nd	nd	del 13q14
18	A	M-CLL	POS	VH1-18*01(FR1)/JH4B	wt	nd	nd	del 11q22, del 13q14
19	B	M-CLL	POS	VH3-7*01	wt	nd	nd	trisomy 12
20	A	M-CLL	POS	VH3-72*01	wt	nd	nd	del 13q14
21	B	M-CLL	NEG	VH3-48*02	nd	nd	nd	del 13q14
22	B	U-CLL	NEG	3-23, 3-21	wt	wt	MUT	del 13q14
23	A	U-CLL	POS	VH4-34*01	wt	nd	nd	trisomy 12, del 17p13
24	C	M-CLL	NEG	VH3-72*01	wt	nd	nd	del 17p13, del 13q14
25	-	M-CLL	NEG	VH3-7*03	wt	nd	nd	del 11q22, del 13q14
26	B	M-CLL	NEG	VH3-23*01	wt	nd	nd	del13q14

- U-CLL and M-CLL : <2% and ≥2% in *IGHV* difference from germline, respectively.
- n.d. not determined
- \* 27%, \*\* 19%, \*\*\* 11%

Figure S1

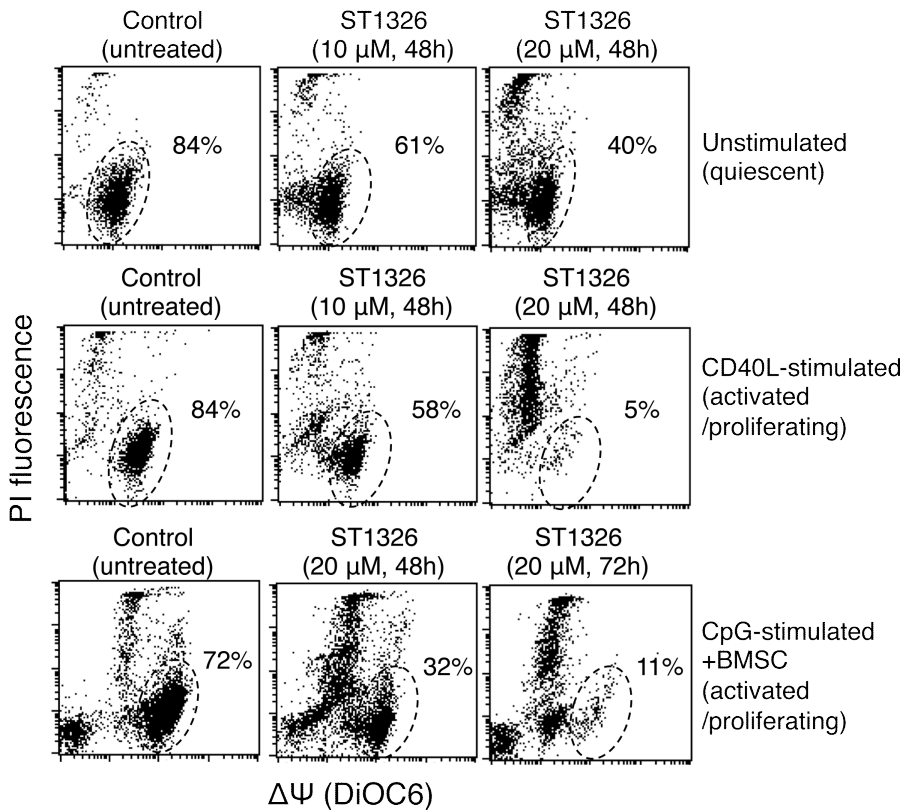


Figure S1:

*Sensitivity to ST1326 of quiescent and activated/proliferating CLL cells.*

Flow cytometric bivariate plots of mitochondrial transmembrane potential ( $\Delta\Psi$ ) as measured by DiOC6 fluorescence, and cell viability, as assessed by PI fluorescence, of leukemic cells from one representative CLL patient. Cells were non-stimulated or stimulated either with CD40L-expressing fibroblasts+IL-4 or CpG+IL-15 (in this sample also in the presence of bone marrow stromal cells, BMSC), and exposed to ST1326 for the times indicated. In stimulated cell cultures, the drug was added at the beginning of stimulation. All controls were measured 48 hours after culture start. Events in the dotted gate are cells with functional  $\Delta\Psi$  and intact plasma membrane. This CLL patient harbors 17p13 deletion.

Figure S2

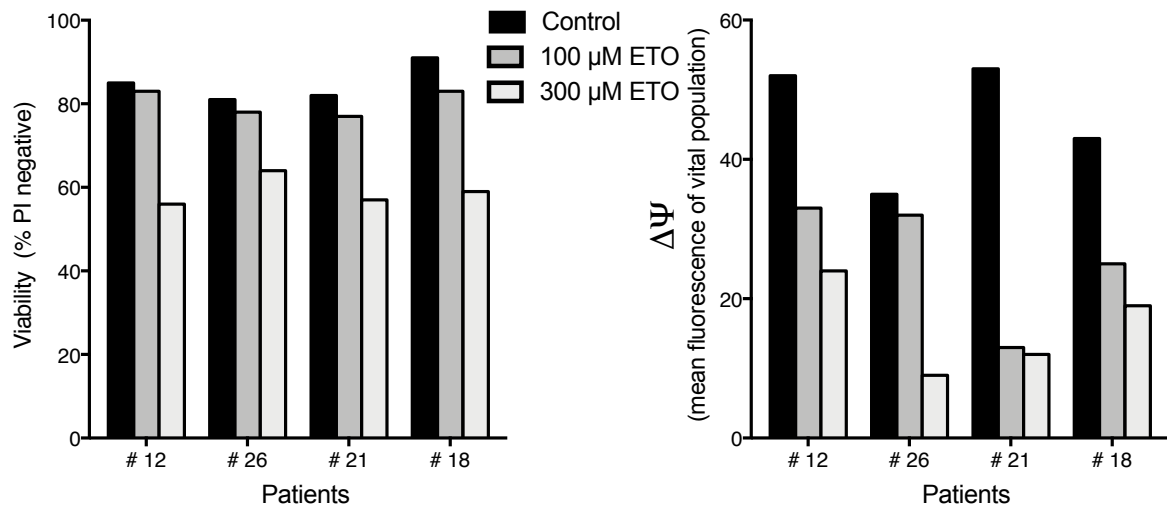


Figure S2:

*Etomoxir is cytotoxic in vitro at ten times higher molarity if compared to ST1326.*

Left: Cell viability assessed flow cytometrically propidium iodide exclusion tests on CD40L+IL4-stimulated cultures of leukemic cells from 4 CLL patients untreated or treated with Etomoxir (48 hours).

Right: Mitochondrial transmembrane potential ( $\Delta\Psi$ ) gated on the vital cell population, as measured by DiOC6 uptake and expressed as flow cytometric fluorescence intensity (MFI) of the PI-excluding cell population (with intact plasma membrane), on same sample as 'left'.

Figure S3

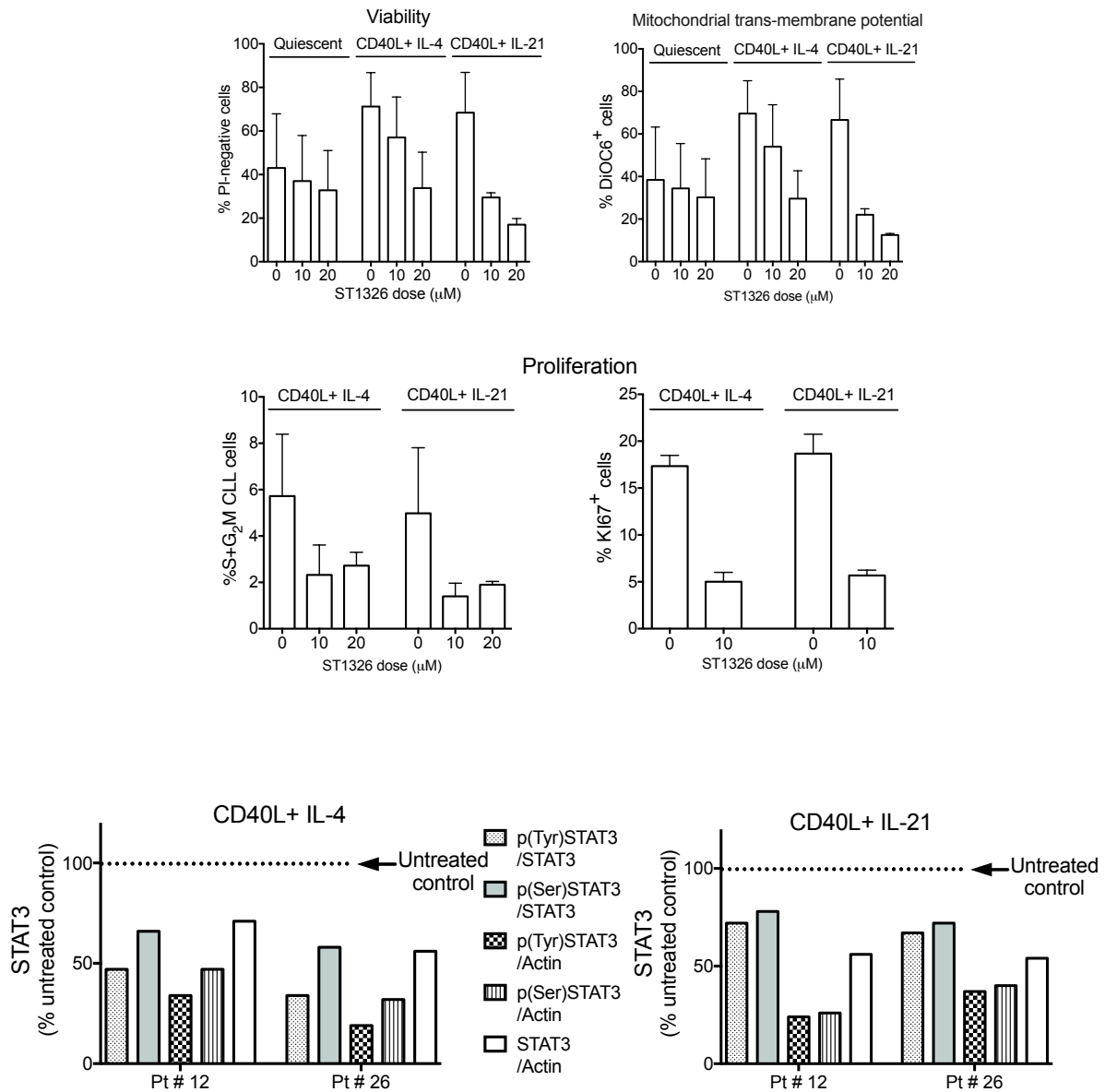


Figure S3:

*ST1326 cytotoxicity in CD40L-stimulated CLL cells sustained either with IL-4 or IL-21.*

ST1326 (at the indicated dose) was administered to cell cultures from 5 CLL patients, stimulated either with CD40L+IL-4 or CD40L+IL-21. Cumulative data of cell viability (n=5),  $\Delta\Psi$  (n=5), cell proliferation (% cells in S+G<sub>2</sub>M cell cycle phases (n=5) and % KI67-positive cells (n=3)) and (p)STAT3 expression (n=2) are reported. For the latter, protein levels in ST1326-treated samples (divided by housekeepers) are calculated as % untreated controls.

Figure S4

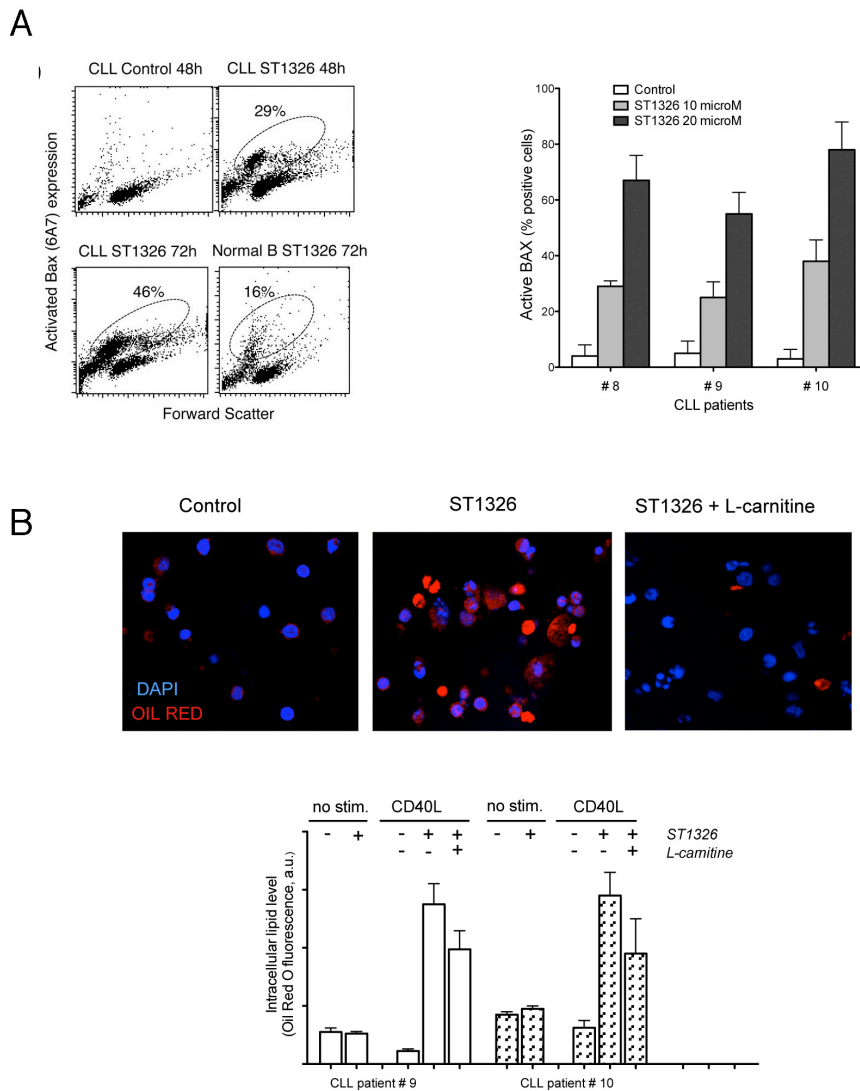


Figure S4

*ST1326 induces Bax activation and intracellular accumulation of lipids that is impaired by exogenous L-carnitine.*

A) Left: Flow cytometric distributions of Forward Light Scatter (FSC)/active-Bax expression, of CD40L+IL-4-stimulated B lymphocytes from one CLL patient and one healthy donor, untreated or treated with ST1326 for the reported times. The percentage of cells expressing the active form of Bax (recognized by the 6A7 antibody) is indicated. Right: data from CLL samples of three CLL patients.

B) Upper: Confocal microscopy images of CLL cells stimulated with CD40L+IL-4-fibroblasts in the absence (left) or presence of ST1326 (10  $\mu$ M, 48 hours), without (middle) or with L-carnitine addition (100  $\mu$ M). Intracellular neutral tryglycerides and lipids are in red (Oil Red O staining) and nuclei in blue (DAPI staining). Lower: intracellular lipid levels as evaluated by fluorescence intensity of Oil Red O-stained cells from two CLL patients. Stimulated CLL cells displayed lower intracellular lipid levels than quiescent cells, possibly reflecting the fatty acid use for de novo membrane synthesis during proliferation.

Figure S5

ST1326-ABT-199 drug combination

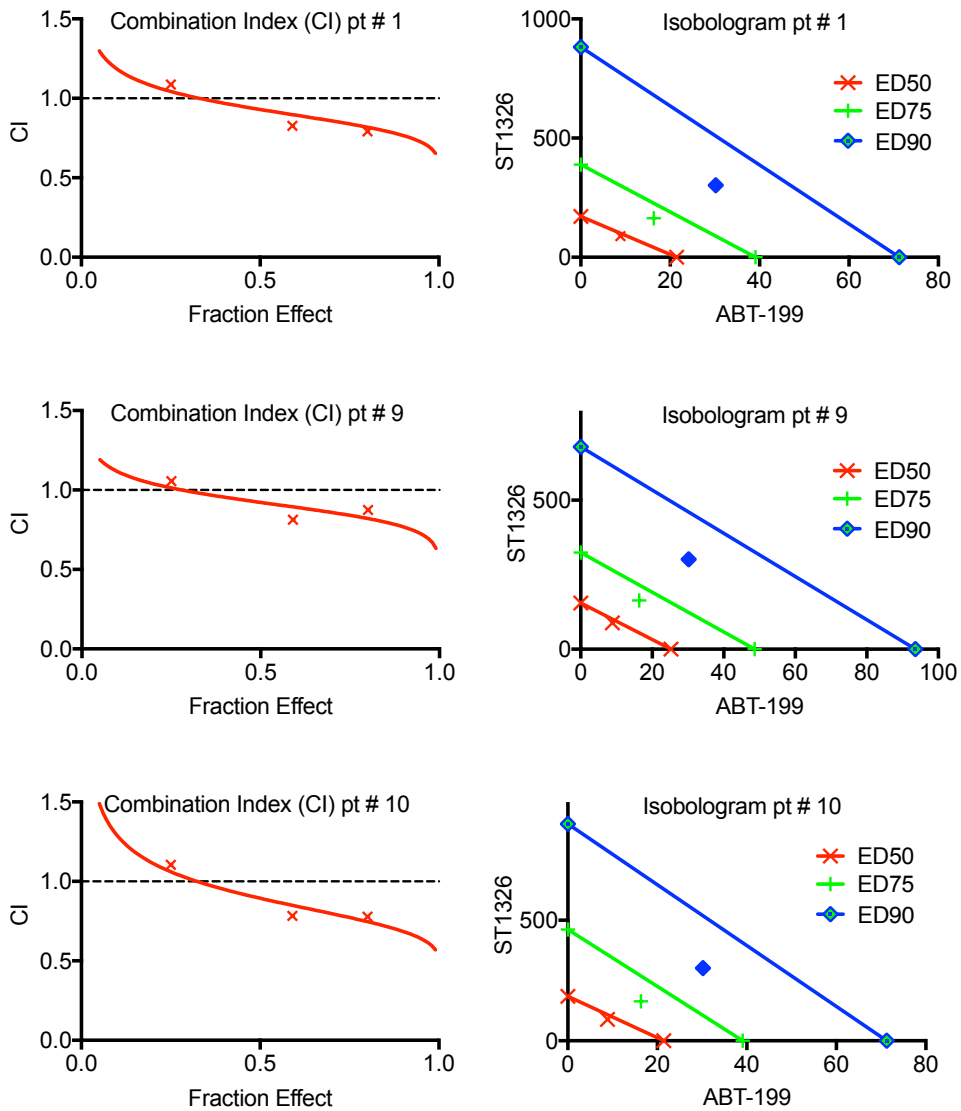


Figure S5:

*Synergic ST1326 and ABT-199 drug combination in activated CLL cells.*

Combination index (CI) curves and isobolograms computed by the Chou–Talalay model (CalcuSyn software, Biosoft, Cambridge) from dose-effect profiles of stimulated CLL cells treated for 24 hours with increasing concentrations of ST1326 (1–10  $\mu\text{M}$ ), ABT-199 (10–100nM for activated samples) or ST1326/ABT-199 at constant ratios. Since CI depends on the ‘fractional effect level’, we report two levels of cytotoxicity, LC75 and LC90 (concentration lethal to 75% and 90% of CLL cells). For each patient one CI and isobologram from one representative experiment are shown. CI measures drug interaction effects: additive:  $0.9 \leq \text{CI} \leq 1.1$ , synergism:  $\text{CI} < 0.9$  and antagonism:  $\text{CI} > 1.1$ . Isobolograms: additive: point on the line, synergism: point below the line, antagonism: point above the line.

Figure S6

### ST1326-Fludarabine drug combination

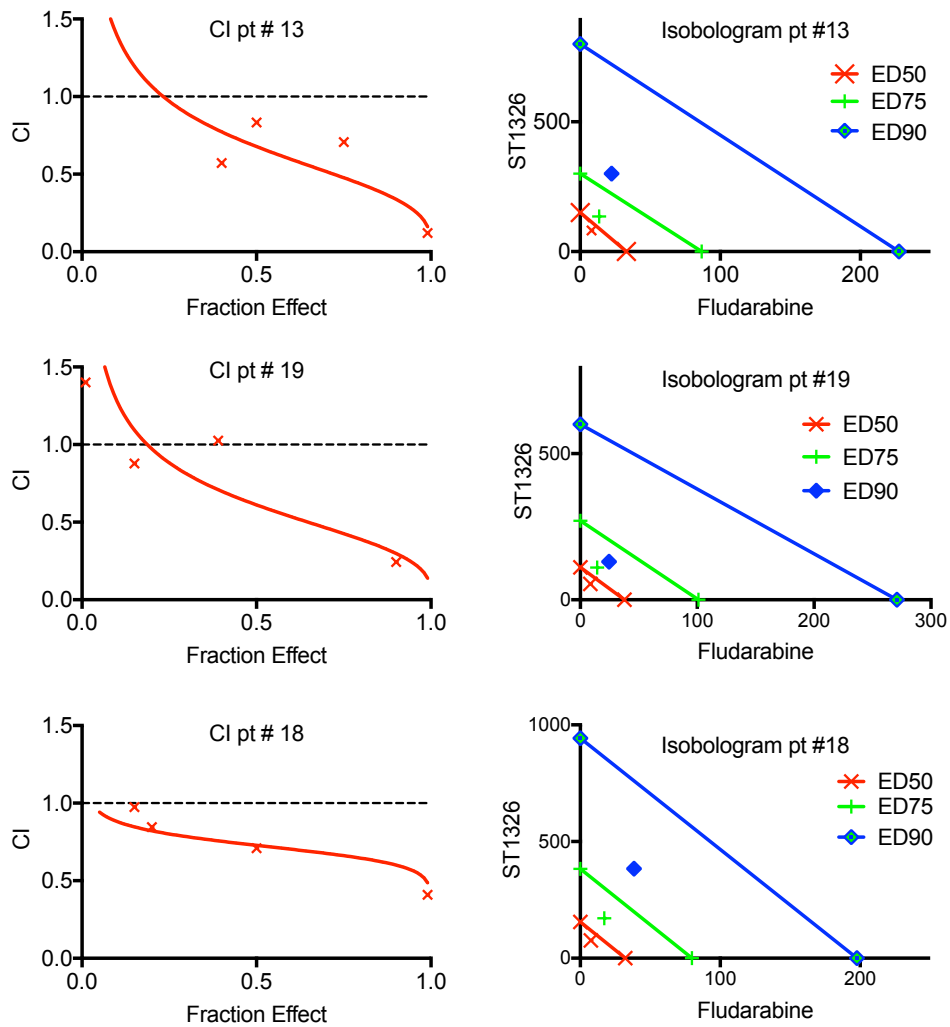


Figure S6:

*Synergic ST1326 and Fludarabine drug combination in activated CLL cells.*

Combination index (CI) curves and isobolograms computed by the Chou–Talalay model (CalcuSyn software, Biosoft, Cambridge) from dose-effect profiles of stimulated CLL cells treated for 24 hours with increasing concentrations of ST1326 (1–10  $\mu\text{M}$ ), ABT-199 (10–100nM for activated samples) or ST1326/ABT-199 at constant ratios. For each patient CI and isobologram from one representative experiment are shown, at LC75 and LC90 level of cytotoxicity.